Mon. Not. R. Astron. Soc. **000**, 000–000 (0000) Printed 4 March 2013 (MN LATEX style file v2.2)

Using Multipoles of the Correlation Function to Measure $H(z)$, $D_A(z)$, and $\beta(z)$ from Sloan Digital Sky Survey Luminous Red Galaxies

Chia-Hsun Chuang,⋆ and Yun Wang

Homer L. Dodge Department of Physics & Astronomy, Univ. of Oklahoma, 440 W Brooks St., Norman, OK 73019, U.S.A.

4 March 2013

ABSTRACT

Galaxy clustering data can be used to measure the cosmic expansion history $H(z)$, the angular-diameter distance $D_A(z)$, and the linear redshift-space distortion parameter $\beta(z)$. Here we present a method for using effective multipoles of the galaxy two-point correlation function ($\hat{\xi}_0(s)$, $\hat{\xi}_2(s)$, $\hat{\xi}_4(s)$, and $\hat{\xi}_6(s)$, with s denoting the comoving separation) to measure $H(z)$, $D_A(z)$, and $\beta(z)$, and validate it using LasDamas mock galaxy catalogs. Our definition of effective multipoles explicitly incorporates the discreteness of measurements, and treats the measured correlation function and its theoretical model on the same footing. We find that for the mock data, $\hat{\xi}_0+\hat{\xi}_2+\hat{\xi}_4$ captures nearly all the information, and gives significantly stronger constraints on $H(z)$, $D_A(z)$, and $\beta(z)$, compared to using only $\hat{\xi}_0+\hat{\xi}_2$.

We apply our method to the sample of luminous red galaxies (LRGs) from the Sloan Digital Sky Survey (SDSS) Data Release 7 (DR7) without assuming a dark energy model or a flat Universe. We find that $\hat{\xi}_4(s)$ deviates on scales of $s < 60\,\mathrm{Mpc}/h$ from the measurement from mock data (in contrast to $\hat{\xi}_0(s)$, $\hat{\xi}_2(s)$, and $\hat{\xi}_6(s)$), leading to a significant difference in the measured mean values of $H(z)$, $D_A(z)$, and $\beta(z)$ from $\hat{\xi}_0+\hat{\xi}_2$ and $\hat{\xi}_0+\hat{\xi}_2+\hat{\xi}_4$, thus it should not be used in deriving parameter constraints. We obtain $\{H(0.35), D_A(0.35), \Omega_m h^2, \beta(z)\}$ = $\{79.6^{+8.3}_{-8.7}\,\mathrm{km\,s^{-1}\,Mpc^{-1}},\ 1057^{+88}_{-87}\mathrm{Mpc},\ 0.103\pm0.015,\ 0.44\pm0.15\}$ using $\hat{\xi}_0+\hat{\xi}_2$. We find that $H(0.35)\,r_s(z_d)/c$ and $D_A(0.35)/r_s(z_d)$ (where $r_s(z_d)$ is the sound horizon at the drag epoch) are more tightly constrained: $\{H(0.35)\,r_s(z_d)/c, D_A(0.35)/r_s(z_d)\}$ = $\{0.0437^{+0.0041}_{-0.0043}, 6.48^{+0.44}_{-0.43}\}$ using $\hat{\xi}_0+\hat{\xi}_2$. We conclude that the multipole method can be used to isolate systematic uncertainties in the data, and provide a useful cross-check of parameter measurements from the full correlation function.

Key words: cosmology: observations, distance scale, large-scale structure of Universe

1 INTRODUCTION

The cosmic large-scale structure from galaxy redshift surveys provides a powerful probe of dark energy and the cosmological model that is highly complementary to the cosmic microwave background (CMB) (Bennett et al. 2003), supernovae (SNe) (Riess et al. 1998; Perlmutter et al. 1999), and weak lensing (Wittman et al. 2000; Bacon, Refregier, & Ellis 2000; Kaiser, Wilson, & Luppino 2000; Van Waerbeke et al. 2000). The scope of galaxy redshift surveys has dramatically increased in the last decade. The PSCz surveyed $\sim 15,000$ galaxies using the Infrared Astronomical Satellite (IRAS) (Saunders et al. 2000), the 2dF Galaxy Redshift Survey (2dFGRS) obtained 221,414 galaxy redshifts (Colless et al. 2001, 2003), and the Sloan Digital Sky Survey (SDSS) has collected 930,000 galaxy spectra in the Seventh Data Release (DR7) (Abazajian et al. 2009). The ongoing galaxy surveys will probe the Universe at higher redshifts; WiggleZ is surveying 240,000 emission-line galaxies at $0.5 < z < 1$ over 1000 square degrees (Blake et al. 2009), and BOSS is surveying 1.5 million luminous red galaxies (LRGs) at $0.1 < z < 0.7$ over 10,000 square degrees (Eisenstein et al. 2011). The planned space mission Euclid[1] will survey over 60 million emission-line galaxies at $0.7 < z < 2$ over 15,000 square degrees (Cimatti et al. 2009; Wang et al. 2010; Laureijs et al. 2011).

Large-scale structure data from galaxy surveys can be analyzed using either the power spectrum or the correlation func-

⋆ E-mail: chuang@nhn.ou.edu

[1] http://www.euclid-emc.org/

tion. Although these two methods are simple Fourier transforms of one another, the analysis processes are quite different and the results cannot be converted using Fourier transform directly because of the finite size of the survey volume. The SDSS data have been analyzed using both the power spectrum method (see, e.g., Tegmark et al. 2004; Hutsi 2005; Padmanabhan et al. 2007; Blake et al. 2007; Percival et al. 2007, 2010; Reid et al. 2010; Montesano et al. 2011), and the correlation function method (see, e.g., Eisenstein et al. 2005; Okumura et al. 2008; Cabre & Gaztanaga 2009; Martinez et al. 2009; Sanchez et al. 2009; Kazin et al. 2010a; Chuang, Wang, & Hemantha 2012; Samushia et al. 2011; Padmanabhan et al. 2012).

The power of galaxy clustering as a dark energy probe lies in the fact that the Hubble parameter, $H(z)$, and the angular diameter distance, $D_A(z)$, can in principle be extracted simultaneously from data through the measurement of the baryon acoustic oscillation (BAO) scale in the radial and transverse directions (Blake & Glazebrook 2003; Seo & Eisenstein 2003; Wang 2006). Okumura et al. (2008) concluded that SDSS DR3 LRG data were not sufficient for measuring $H(z)$ and $D_A(z)$; they derived constraints on cosmological parameters assuming that dark energy is a cosmological constant. Cabre & Gaztanaga (2009) measured the linear redshift space distortion parameter β, galaxy bias, and σ_8 from SDSS DR6 LRGs. Gaztanaga, Cabre, & Hui (2009) obtained a measurement of $H(z)$ by measuring the peak of the 2PCF along the line of sight. However, Kazin et al. (2010b) showed that the amplitude of the line-of-sight peak is consistent with sample variance.

In our previous paper (Chuang & Wang 2011), we presented the method to measure $H(z)$ and $D_A(z)$ from the full 2D correlation function of a sample of SDSS DR7 LRGs (Eisenstein et al. 2001) without assuming a dark energy model or a flat Universe. It is also the first application which includes the geometric distortion (also known as Alcock-Paczynski test (Alcock & Paczynski 1979)) on the galaxy clustering data at large scales. We demonstrated the feasibility of extracting $H(z)$ and $D_A(z)$ by applying the method on the individual LasDamas mock catalogs which mimic the galaxy sample and survey geometry of the observational data we used. In this paper, we extend our method by exploring the use of the multipoles of the correlation function to measure $H(z)$, $D_A(z)$, and $\beta(z)$. The obvious advantage of using multipoles of the correlation function instead of the full 2D correlation function is the reduced number of data points used to obtain similar amount of information. In Section 2, we introduce the galaxy sample used in our study. In Section 3, we describe the details of our method. In Section 4, we present our results. In Sectioin 5, we apply some systematic tests to our measurements. We summarize and conclude in Sec. 6.

2 DATA

The SDSS has observed one-quarter of the entire sky and performed a redshift survey of galaxies, quasars and stars in five passbands $u, g, r, i,$ and z with a 2.5m telescope (Fukugita et al. 1996; Gunn et al. 1998, 2006). We use the public catalog, the NYU Value-Added Galaxy Catalog (VAGC) (Blanton et al. 2005), derived from the SDSS II final public data release, Data Release 7 (DR7) (Abazajian et al. 2009). We select our LRG sample from the NYU VAGC with the flag $primTarget$ bit mask set to 32. K-corrections have been applied to the galaxies with a fiducial model (ΛCDM with $\Omega_m = 0.3$ and $h = 1$), and the selected galaxies are required to have rest-frame g-band absolute magnitudes $-23.2 < M_g < -21.2$ (Blanton & Roweis 2007). The same selection criteria were used in previous papers (Zehavi et al. 2005; Eisenstein et al. 2005; Okumura et al. 2008; Kazin et al. 2010a). The sample we use is referred to as "DR7full" in Kazin et al. (2010a). Our sample includes 87000 LRGs in the redshift range 0.16-0.44.

Spectra cannot be obtained for objects closer than 55 arcsec within a single spectroscopic tile due to the finite size of the fibers. To correct for these "collisions", the redshift of an object that failed to be measured would be assigned to be the same as the nearest successfully observed one. Both fiber collision corrections and K-corrections have been made in NYU-VAGC (Blanton et al. 2005). The collision corrections applied here are different from what has been suggested in Zehavi et al. (2005). However, the effect should be small since we are using relatively large scale which are less affected by the collision corrections.

We construct the radial selection function as a cubic spline fit to the observed number density histogram with the width $\Delta z = 0.01$. The NYU-VAGC provides the description of the geometry and completeness of the survey in terms of spherical polygons. We adopt it as the angular selection function of our sample. We drop the regions with completeness below 60% to avoid unobserved plates (Zehavi et al. 2005). The Southern Galactic Cap region is also dropped.

3 METHODOLOGY

In this section, we describe the measurement of the multipoles of the correlation function from the observational data, construction of the theoretical prediction, and the likelihood analysis that leads to constraints on dark energy and cosmological parameters.

3.1 Measuring the Two-Dimensional Two-Point Correlation Function

We convert the measured redshifts of galaxies to comoving distances by assuming a fiducial model, ΛCDM with $\Omega_m = 0.25$. We use the two-point correlation function estimator given by Landy & Szalay (1993):

$$\xi(\sigma,\pi) = \frac{DD(\sigma,\pi) - 2DR(\sigma,\pi) + RR(\sigma,\pi)}{RR(\sigma,\pi)}, \quad (1)$$

where π is the separation along the line of sight (LOS), σ is the separation in the plane of the sky, DD, DR, and RR represent the normalized data-data, data-random, and random-random pair counts respectively in a distance range. The LOS is defined as the direction from the observer to the center of a pair. The bin size we use here is $1\,h^{-1}$Mpc$\times 1\,h^{-1}$Mpc. The Landy and Szalay estimator has minimal variance for a Poisson process. Random data are generated with the same radial and angular selection functions as the real data. One can reduce the shot noise due to random data by increasing the number of random data. The number of random data we use is 10 times that of the real data. While calculating the pair counts, we assign to each data point a radial weight of $1/[1 + n(z) \cdot P_w]$, where $n(z)$ is the radial selection function and $P_w = 4 \cdot 10^4\ h^{-3}$Mpc^3 (Eisenstein et al. 2005).

3.2 Theoretical Two-Dimensional Two-Point Correlation Function

We compute the linear power spectra by using CAMB (Lewis, Challinor, & Lasenby 2000). To include the effect of non-

linear structure formation on the BAOs, we first calculate the dewiggled power spectrum

$$P_{dw}(k) = P_{lin}(k)\exp\left(-\frac{k^2}{2k_\star^2}\right)+P_{nw}(k)\left[1-\exp\left(-\frac{k^2}{2k_\star^2}\right)\right], \quad (2)$$

where $P_{lin}(k)$ is the linear matter power spectrum, $P_{nw}(k)$ is the no-wiggle or pure CDM power spectrum calculated using Eq.(29) from Eisenstein & Hu (1998), and $k_\star$ is marginalized over with a flat prior over the range of 0.09 to 0.13.

We then use the software package *halofit* (Smith et al. 2003) to compute the non-linear matter power spectrum:

$$r_{halofit}(k) \equiv \frac{P_{halofit,nw}(k)}{P_{nw}(k)} \quad (3)$$

$$P_{nl}(k) = P_{dw}(k) r_{halofit}(k), \quad (4)$$

where $P_{halofit,nw}(k)$ is the power spectrum obtained by applying halofit to the no-wiggle power spectrum, and $P_{nl}(k)$ is the non-linear power spectrum. We compute the theoretical real space two-point correlation function, $\xi(r)$, by Fourier transforming the non-linear power spectrum $P_{nl}(k)$.

In the linear regime (i.e., large scales) and adopting the small-angle approximation (which is valid on scales of interest), the 2D correlation function in the redshift space can be written as (Kaiser 1987; Hamilton 1992)

$$\xi^\star(\sigma,\pi) = \xi_0(s)P_0(\mu) + \xi_2(s)P_2(\mu) + \xi_4(s)P_4(\mu), \quad (5)$$

where $s = \sqrt{\sigma^2+\pi^2}$, μ is the cosine of the angle between $\mathbf{s} = (\sigma,\pi)$ and the LOS, and P_l are Legendre polynomials. The multipoles of ξ are defined as

$$\xi_0(r) = \left(1+\frac{2\beta}{3}+\frac{\beta^2}{5}\right)\xi(r), \quad (6)$$

$$\xi_2(r) = \left(\frac{4\beta}{3}+\frac{4\beta^2}{7}\right)[\xi(r)-\bar{\xi}(r)], \quad (7)$$

$$\xi_4(r) = \frac{8\beta^2}{35}\left[\xi(r)+\frac{5}{2}\bar{\xi}(r)-\frac{7}{2}\bar{\bar{\xi}}(r)\right], \quad (8)$$

where β is the redshift space distortion parameter and

$$\bar{\xi}(r) = \frac{3}{r^3}\int_0^r \xi(r')r'^2 dr', \quad (9)$$

$$\bar{\bar{\xi}}(r) = \frac{5}{r^5}\int_0^r \xi(r')r'^4 dr'. \quad (10)$$

Next, we convolve the 2D correlation function with the distribution function of random pairwise velocities, $f(v)$, to obtain the final model $\xi(\sigma,\pi)$ (Peebles 1980)

$$\xi(\sigma,\pi) = \int_{-\infty}^{\infty}\xi^\star\left(\sigma,\pi-\frac{v}{H(z)a(z)}\right)f(v)dv, \quad (11)$$

where the random motions are represented by an exponential form (Ratcliffe et al. 1998; Landy 2002)

$$f(v) = \frac{1}{\sigma_v\sqrt{2}}\exp\left(-\frac{\sqrt{2}|v|}{\sigma_v}\right), \quad (12)$$

where σ_v is the pairwise peculiar velocity dispersion.

The parameter set we use to compute the theoretical correlation function is $\{H(z), D_A(z), \beta, \Omega_m h^2, \Omega_b h^2, n_s, \sigma_v, k_\star\}$, where Ω_m and Ω_b are the density fractions of matter and baryons, n_s is the powerlaw index of the primordial matter power spectrum, and h is the dimensionless Hubble constant ($H_0 = 100h$ km s^{-1}Mpc^{-1}). We set $h = 0.7$ while calculating the non-linear power spectra. On the scales we use for comparison with data, the theoretical correlation function only depends on cosmic curvature and dark energy through parameters $H(z)$, $D_A(z)$, and $\beta(z)$, assuming that dark energy perturbations are unimportant (valid in simplest dark energy models). Thus we are able to extract constraints from data that are independent of a dark energy model and cosmic curvature.

3.3 Effective Multipoles of the Correlation Function

From Eqs.(5) and (11), we find that

$$\begin{aligned}\hat{\xi}_l(s) &\equiv \int_{-\infty}^{\infty} \mathrm{d}v f(v)\,\xi_l\left(\sqrt{\sigma^2+\left[\pi-\frac{v}{H(z)a(z)}\right]^2}\right)\\ &= \frac{2l+1}{2}\int_{-1}^{1}\mathrm{d}\mu\,\xi(\sigma,\pi)P_l(\mu)\\ &= \frac{2l+1}{2}\int_0^{\pi}\mathrm{d}\theta\,\sqrt{1-\mu^2}\,\xi(\sigma,\pi)P_l(\mu), \end{aligned} \quad (13)$$

where $\mu = \cos\theta$, and $P_l(\mu)$ is the Legendre Polynomial (l =0, 2, 4, and 6 here). Note that we are integrating over a spherical shell with radius s, while actual measurements of $\xi(\sigma,\pi)$ are done in discrete bins. To compare the measured $\xi(\sigma,\pi)$ and its theoretical model on the same footing, we convert the last integral in Eq.(13) into a sum. This leads to our definition for the effective multipoles of the correlation function:

$$\hat{\xi}_l(s) \equiv \frac{\sum_{s-\frac{\Delta s}{2}<\sqrt{\sigma^2+\pi^2}<s+\frac{\Delta s}{2}} (2l+1)\xi(\sigma,\pi)P_l(\mu)\sqrt{1-\mu^2}}{\text{Number of bins used in the numerator}}, \quad (14)$$

where $\Delta s = 5\,h^{-1}$Mpc in this work, and

$$\sigma = (n+\frac{1}{2})h^{-1}\text{Mpc}, n = 0,1,2,... \quad (15)$$

$$\pi = (m+\frac{1}{2})h^{-1}\text{Mpc}, m = 0,1,2,... \quad (16)$$

$$\mu \equiv \frac{\pi}{\sqrt{\sigma^2+\pi^2}}. \quad (17)$$

Note that both the measurements and the theoretical predictions for the effective multipoles are computed using Eq.(14), with $\xi(\sigma,\pi)$ given by the measured correlation function (see Eq.(1)) for the measured effective multipoles, and Eqs.(5)-(11) for their theoretical predictions. We do not use the conventional definitions of multipoles to extract parameter constraints as they use continous integrals. Bias could be introduced if the definitions of multipoles are diffirent between measurements from data and the theoretical model.

3.4 Covariance Matrix

We use the 160 mock catalogs from the LasDamas simulations[2] (McBride et al., in preparation) to estimate the covariance matrix of the observed correlation function. LasDamas provides mock catalogs matching SDSS main galaxy and LRG samples. We use the LRG mock catalogs from the LasDamas gamma release with the same cuts as the SDSS LRG DR7full sample, $-23.2 < M_g < -21.2$ and $0.16 < z < 0.44$. We have diluted the mock catalogs to

[2] http://lss.phy.vanderbilt.edu/lasdamas/

match the radial selection function of the observational data by randomly selecting the mock galaxies according to the number density of the data sample. We calculate the multipoles of the correlation functions of the mock catalogs and construct the covariance matrix as

$$C_{ij} = \frac{1}{N-1}\sum_{k=1}^{N}(\bar{X}_i - X_i^k)(\bar{X}_j - X_j^k), \tag{18}$$

where N is the number of the mock catalogs, $\bar{X}_m$ is the mean of the m^{th} element of the vector from the mock catalog multipoles, and X_m^k is the value in the m^{th} elements of the vector from the k^{th} mock catalog multipoles. The data vector $\mathbf{X}$ is defined by

$$\mathbf{X} = \{\hat{\xi}_0^{(1)}, \hat{\xi}_0^{(2)}, ..., \hat{\xi}_0^{(N)}; \hat{\xi}_2^{(1)}, \hat{\xi}_2^{(2)}, ..., \hat{\xi}_2^{(N)}; ...\}, \tag{19}$$

where N is the number of data points in each measured multipole; $N = 16$ in this work. The length of the data vector $\mathbf{X}$ depends on how many multipoles are used.

3.5 Likelihood

The likelihood is taken to be proportional to $\exp(-\chi^2/2)$ (Press et al. 1992), with χ^2 given by

$$\chi^2 \equiv \sum_{i,j=1}^{N_X}\left[X_{th,i} - X_{obs,i}\right] C_{ij}^{-1}\left[X_{th,j} - X_{obs,j}\right] \tag{20}$$

where N_X is the length of the vector used, X_{th} is the vector from the theoretical model, and X_{obs} is the vector from the observational data.

As explained in Chuang & Wang (2011), instead of recalculating the observed correlation function for different theoretical models, we rescale the theoretical correlation function to avoid rendering χ^2 values arbitrary. The rescaled theoretical correlation function is computed by

$$T^{-1}(\xi_{th}(\sigma,\pi)) = \xi_{th}\left(\frac{D_A(z)}{D_A^{fid}(z)}\sigma, \frac{H^{fid}(z)}{H(z)}\pi\right), \tag{21}$$

where ξ_{th} is given by eq. (11). Hence χ^2 can be rewrited as

$$\chi^2 \equiv \sum_{i,j=1}^{N_X}\left\{T^{-1}X_{th,i} - X_{obs,i}^{fid}\right\} C_{fid,ij}^{-1} \cdot \cdot\left\{T^{-1}X_{th,j} - X_{obs,j}^{fid}\right\}, \tag{22}$$

where $T^{-1}X_{th}$ is a vector given by eq. (21) with ξ_{th} replaced by its effective multipoles (defined by eq. (14)), and X_{obs}^{fid} is the corresponding vector from observational data measured assuming the fiducial model in converting redshifts to distances. See Chuang & Wang (2011) for a more detailed description of our rescaling method.

3.6 Markov Chain Monte-Carlo Likelihood Analysis

We use CosmoMC in a Markov Chain Monte-Carlo likelihood analysis (Lewis & Bridle 2002). The parameter space that we explore spans the parameter set of $\{H(0.35)$, $D_A(0.35)$, $\Omega_m h^2$, β, $\Omega_b h^2$, n_s, σ_v, $k_\star\}$. Only $\{H(0.35)$, $D_A(0.35)$, $\Omega_m h^2$, $\beta\}$ are well constrained using SDSS LRGs alone in the scale range interested. We marginalize over the other parameters, $\{\Omega_b h^2$, n_s, σ_v, $k_\star\}$, with the flat priors, $\{(0.01859, 0.02657)$, $(0.865, 1.059)$, $(0, 500)\mathrm{s}^{-1}\mathrm{km}$, $(0.09, 0.13)h\mathrm{Mpc}^{-1}\}$, where the flat priors of $\Omega_b h^2$ and n_s are centered on the measurements from WMAP7 and has width of $\pm 7\sigma_{WMAP}$ (with σ_{WMAP} from Komatsu et al. (2010)). These priors are wide enough to ensure that CMB constraints are not double counted when our results are combined with CMB data (Chuang, Wang, & Hemantha 2012). We also marginalize over the amplitude of the galaxy correlation function, effectively marginalizing over a linear galaxy bias.

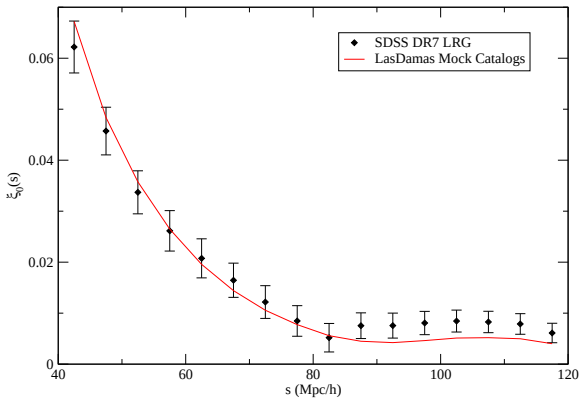

Figure 1. Measurement of monopole of the correlation function of the SDSS DR7 LRG (diamond data points) comparing to the averaged monopole of the correlation functions of the mock catalogs (solid line). The error bars are taken as the square roots of the diagnal elements of the covariance matrix.

4 RESULTS

4.1 Measurement of multipoles

Fig.1, 2, 3, and 4 show the effective monopole ($\hat{\xi}_0$), quadrupole ($\hat{\xi}_2$), hexadecapole ($\hat{\xi}_4$), and hexacontatetrapole ($\hat{\xi}_6$) of measured from SDSS LRGs compared with the averaged effetive multipoles measured from the mock catalogs. We are using the same scale range as Chuang & Wang (2011) ($s = 40-120\,h^{-1}$Mpc) for comparison and the bin size used is 5 h^{-1}Mpc. The data points from the multipoles in the scale range considered are combined to form a vector, $\mathbf{X}$ (see equation(19)).

We find that $\xi_4(s)$ deviates on scales of $s < 60\,\mathrm{Mpc}/h$ from the measurement from mock data (in contrast to $\xi_0(s)$, $\xi_2(s)$, and $\xi_6(s)$), leading to a significant difference in the measured mean values of $H(z)$, $D_A(z)$, and $\beta(z)$ from $\xi_0 + \xi_2$ and $\xi_0 + \xi_2 + \xi_4$, thus it should not be used in deriving parameter constraints.

A frequently used combination of the monopole and the quadupole is the normalized quadrupole, defined by

$$Q(s) = \frac{\xi_2(s)}{\xi_0(s) - (3/s^3)\int_0^s \xi_0(s')s'^2 ds'}. \tag{23}$$

For comparison with previous work, we measure the effective normalized quadrupole defined by

$$\hat{Q}(s) \equiv \frac{\hat{\xi}_2(s)}{\hat{\xi}_0(s) - (3/s^3)\sum_{0<s'\leqslant s}\hat{\xi}_0(s')s'^2\Delta s}, \tag{24}$$

from SDSS LRGs and show it in Fig.5. It is in good agreement with

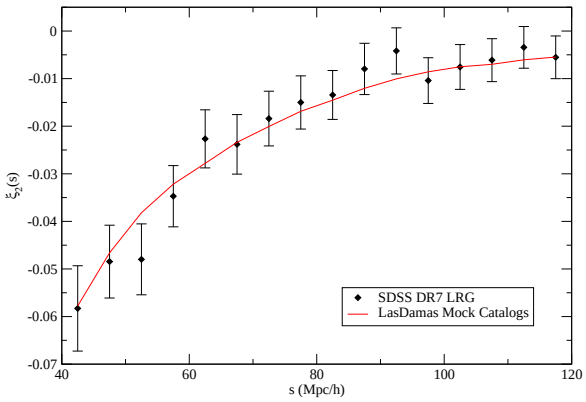

Figure 2. Measurement of quadrupole of the correlation function of the SDSS DR7 LRG (diamond data points) comparing to the averaged quadrupole of the correlation functions of the mock catalogs (solid line). The error bars are taken as the square roots of the diagnal elements of the covariance matrix.

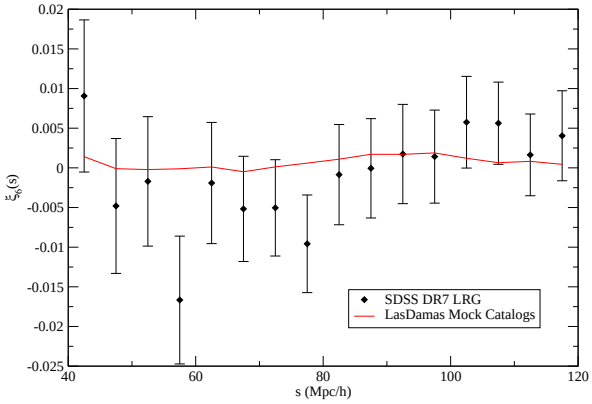

Figure 4. Measurement of hexacontatetrapole of the correlation function of the SDSS DR7 LRG (diamond data points) comparing to the averaged hexacontatetrapole of the correlation functions of the mock catalogs (solid line). The error bars are taken as the square roots of the diagnal elements of the covariance matrix.

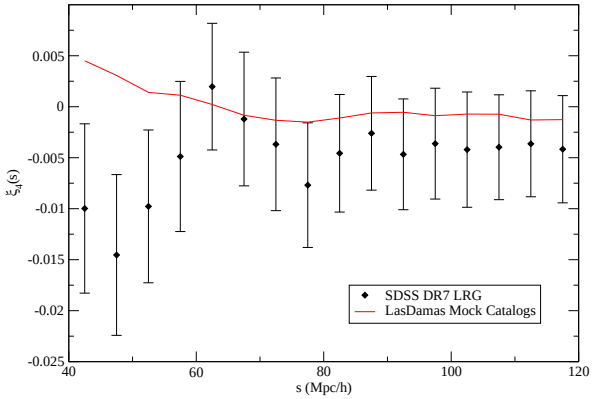

Figure 3. Measurement of hexadecapole of the correlation function of the SDSS DR7 LRG (diamond data points) comparing to the averaged hexadecapole of the correlation functions of the mock catalogs (solid line). The error bars are taken as the square roots of the diagnal elements of the covariance matrix.

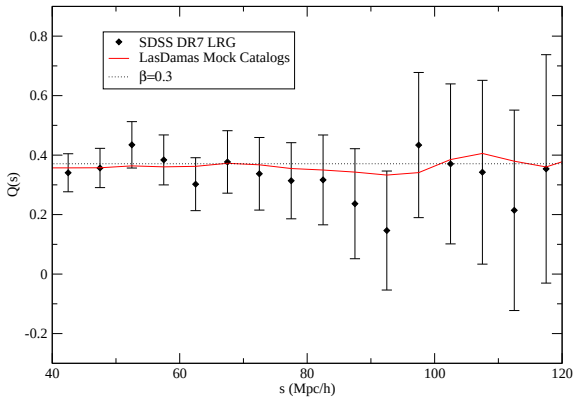

Figure 5. Measurement of the normalized quadrupole from the SDSS DR7 LRG (diamond data points) comparing to the mean measurement from the mock catalogs (solid line). The error bars are taken as the square roots of the diagnal elements of the covariance matrix. Dashed line is the theoretical prediction for $beta = 0.3$ assuming linear power spectrum and small-angle approximation.

the expectation from the LasDamas mocks, as well as with previous work by Samushia et al. (2011).

4.2 Measurement of $\{H(0.35)$, $D_A(0.35)$, $\beta(0.35)\}$

,

We now present the model independent measurements of the parameters $\{H(0.35),\ D_A(0.35),\ \Omega_m h^2, \beta\}$, obtained by using the method described in previous sections. We also present the derived parameters including $H(0.35)\, r_s(z_d)/c$ and $D_A(0.35)/r_s(z_d)$ which have tigher constraints.

First, we apply our method of using multipoles of the correlation function to the individual LasDamas mock catalogs and find that our measurements are consistent with the input parameters of the simulations and also the results from using full 2D 2PCF. We also find that the constraints from using monopole + quadrupole + hexadecapole is almost as good as using full 2D correlation function, but using extra hexacontatetrapole does not provide significant improvement to the constraints. Then, we apply our method on the observational data. Finally, we compare our results with other previous work by restricting our method to the same conditions accordingly.

	mean	σ	input value
$H(0.35)$	81.1	5.6	81.79
$D_A(0.35)$	1017	63	1032.8
$\Omega_m h^2$	0.119	0.014	0.1225
β	0.325	0.076	–
$H(0.35)\, r_s(z_d)/c$	0.0436	0.0030	0.0434
$D_A(0.35)/r_s(z_d)$	6.29	0.36	6.48

Table 1. The mean and standard deviation of the distribution of the measured values of $\{H(0.35),\ D_A(0.35),\ \Omega_m h^2,\ \beta,\ H(0.35)\, r_s(z_d)/c,\ D_A(0.35)/r_s(z_d)\}$ from each monopole + quadrupole ($\hat{\xi}_0 + \hat{\xi}_2$) of 40 LasDamas mock catalogs (which are indexed with 01a-40a). Our measurements are consistent with the input values within 1σ, where each σ is computed from the 40 means measured from the 40 mock catalogs. The unit of H is $\mathrm{km\,s^{-1}\,Mpc^{-1}}$. The unit of D_A and $r_s(z_d)$ is Mpc.

4.2.1 *Validation Using Mock Catalogs*

In order to validate our method, we have applied it to the first 40 LasDamas mock catalogs (which are indexed with 01a-40a)[3]. Again, we apply the flat and wide priors ($\pm 7\sigma_{WMAP7}$) on $\Omega_b h^2$ and n_s, centered on the input values of the simulation ($\Omega_b h^2 = 0.0196$ and $n_s = 1$).

Table 1 shows the means and standard deviations of the distributions of our measurements of $\{H(0.35),\ D_A(0.35),\ \Omega_m h^2,\ \beta,\ H(0.35)\, r_s(z_d)/c,\ D_A(0.35)/r_s(z_d)\}$ from each monopole + quadrupole ($\hat{\xi}_0 + \hat{\xi}_2$) of the LasDamas mock catalogs of the SDSS LRG sample. Table 2 and 3 show the measurements using monopole + quadrupole + hexadecapole ($\hat{\xi}_0 + \hat{\xi}_2 + \hat{\xi}_4$) and monopole + quadrupole + hexadecapole + hexacontatetrapole ($\hat{\xi}_0 + \hat{\xi}_2 + \hat{\xi}_4 + \hat{\xi}_6$) respectively. For comparison, Table 4 shows the results using full 2D method from Chuang & Wang (2011), but we are using only 40 for this study instead of 80 mock catalogs. These are consistent with the input parameters, establishing the validity of our method.

While the constraints from using $\hat{\xi}_0 + \hat{\xi}_2 + \hat{\xi}_4$ are significantly tighter than using $\hat{\xi}_0 + \hat{\xi}_2$, the constraints from using $\hat{\xi}_0 + \hat{\xi}_2 + \hat{\xi}_4 + \hat{\xi}_6$ are nearly the same as that from using $\hat{\xi}_0 + \hat{\xi}_2 + \hat{\xi}_4$. This indicates that $\hat{\xi}_0 + \hat{\xi}_2 + \hat{\xi}_4$ captures nearly all of the information that can be extracted from the data given the noise level. In principle, one could obtain better constraints by including more multipoles. However, the tradeoff is introduing noise to the covariance matrix which could be a problem, since the number of the mock catalogs used to construct the covariance matrix is not big enough. We also show the measurements of $H(0.35)\, r_s(z_d)/c$, $D_A(0.35)/r_s(z_d)$, $\Omega_m h^2$, and β of each mock catalog in Fig. 6, Fig. 7, Fig. 8, and Fig. 9 to show the scattering among different mock catalogs and the deviations among different methods. One can see the measurements among different methods are consistent for most mock catalogs, but there are still some obvious deviations ($> 1\sigma$) for a few cases.

An important point to note is that since the mock data do not include unknown systematic effects, the mean values of estimated parameters remain nearly unchanged as more multipoles measured from data are added to the analysis and the parameter constraints are tightened with the addition of information.

[3] We only use 40 instead of 160 mock catalogs because the MCMC is computationlly expensive. However, the covariance matrix is contructed with 160 mock catalogs.

	mean	σ	input value
$H(0.35)$	80.4	4.9	81.79
$D_A(0.35)$	1027	56	1032.8
$\Omega_m h^2$	0.116	0.013	0.1225
β	0.327	0.066	–
$H(0.35)\, r_s(z_d)/c$	0.0435	0.0025	0.0434
$D_A(0.35)/r_s(z_d)$	6.31	0.31	6.48

Table 2. The mean and standard deviation of the distribution of the measured values of $\{H(0.35),\ D_A(0.35),\ \Omega_m h^2,\ \beta,\ H(0.35)\, r_s(z_d)/c,\ D_A(0.35)/r_s(z_d)\}$ from each monopole + quadrupole + hexadecapole ($\hat{\xi}_0 + \hat{\xi}_2 + \hat{\xi}_4$) of 40 LasDamas mock catalogs (which are indexed with 01a-40a). Our measurements are consistent with the input values within 1σ, where each σ is computed from the 40 means measured from the 40 mock catalogs. The unit of H is $\mathrm{km\,s^{-1}\,Mpc^{-1}}$. The unit of D_A and $r_s(z_d)$ is Mpc.

	mean	σ	input value
$H(0.35)$	80.3	5.1	81.79
$D_A(0.35)$	1021	48	1032.8
$\Omega_m h^2$	0.116	0.013	0.1225
β	0.324	0.075	–
$H(0.35)\, r_s(z_d)/c$	0.0434	0.0026	0.0434
$D_A(0.35)/r_s(z_d)$	6.28	0.26	6.48

Table 3. The mean and standard deviation of the distribution of the measured values of $\{H(0.35),\ D_A(0.35),\ \Omega_m h^2,\ \beta,\ H(0.35)\, r_s(z_d)/c,\ D_A(0.35)/r_s(z_d)\}$ from each monopole + quadrupole + hexadecapole + hexacontatetrapole ($\hat{\xi}_0 + \hat{\xi}_2 + \hat{\xi}_4 + \hat{\xi}_6$) of 40 LasDamas mock catalogs (which are indexed with 01a-40a). Our measurements are consistent with the input values within 1σ, where each σ is computed from the 40 means measured from the 40 mock catalogs. The unit of H is $\mathrm{km\,s^{-1}\,Mpc^{-1}}$. The unit of D_A and $r_s(z_d)$ is Mpc.

4.2.2 *Measurements from SDSS DR7 LRG*

Table 5 lists the mean, rms variance, and 68% confidence level limits of the parameters, $\{H(0.35),\ D_A(0.35),\ \Omega_m h^2,\ \beta,\ H(0.35)\, r_s(z_d)/c,\ D_A(0.35)/r_s(z_d)\}$, derived in an MCMC likelihood analysis from the measured $\hat{\xi}_0 + \hat{\xi}_2$ of the correlation function of the SDSS LRG sample. Table 6 lists the mean, rms variance,

	mean	σ	input value
$H(0.35)$	80.5	4.0	81.79
$D_A(0.35)$	1026	54	1032.8
$\Omega_m h^2$	0.117	0.013	0.1225
β	0.353	0.060	–
$H(0.35)\, r_s(z_d)/c$	0.0435	0.0021	0.0434
$D_A(0.35)/r_s(z_d)$	6.31	0.26	6.48

Table 4. The mean and standard deviation of the distribution of the measured values of $\{H(0.35),\ D_A(0.35),\ \Omega_m h^2,\ \beta,\ H(0.35)\, r_s(z_d)/c,\ D_A(0.35)/r_s(z_d)\}$ from each 2D 2PCF of 40 LasDamas mock catalogs (which are indexed with 01a-40a). Our measurements are consistent with the input values within 1σ, where each σ is computed from the 40 means measured from the 40 mock catalogs. The unit of H is $\mathrm{km\,s^{-1}\,Mpc^{-1}}$. The unit of D_A and $r_s(z_d)$ is Mpc.

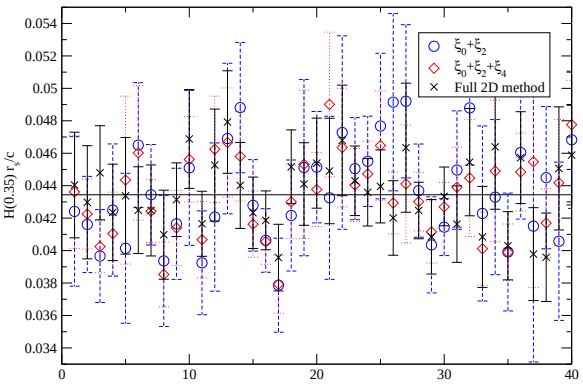

Figure 6. Measurements of the means and standard deviation of $H(0.35)\,r_s(z_d)/c$ from 40 individual mock catalogs (indexed as 01a to 40a). The blue circles show the measurements using $\hat{\xi}_0+\hat{\xi}_2$. The red dinmonds show the measurements using $\hat{\xi}_0+\hat{\xi}_2+\hat{\xi}_4$. The black crosses show the measurements using full 2D 2PCF method from our previous work. The black line shows the theoretical value computed with the input parameters of the simulations.

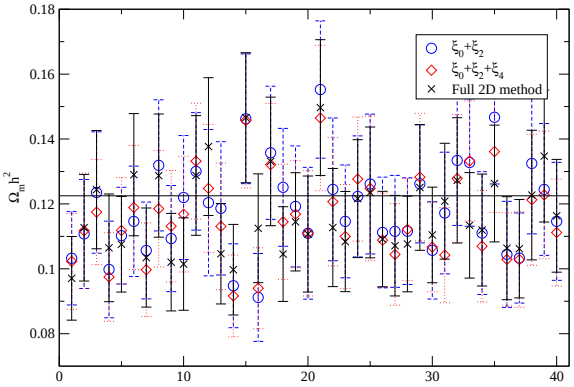

Figure 8. Measurements of the means of $\Omega_m h^2$ from 40 individual mock catalogs (indexed as 01a to 40a). The blue circles show the measurements using $\hat{\xi}_0+\hat{\xi}_2$. The red dinmonds show the measurements using $\hat{\xi}_0+\hat{\xi}_2+\hat{\xi}_4$. The black crosses show the measurements using full 2D 2PCF method from our previous work. The black line shows the theoretical value computed with the input parameters of the simulations.

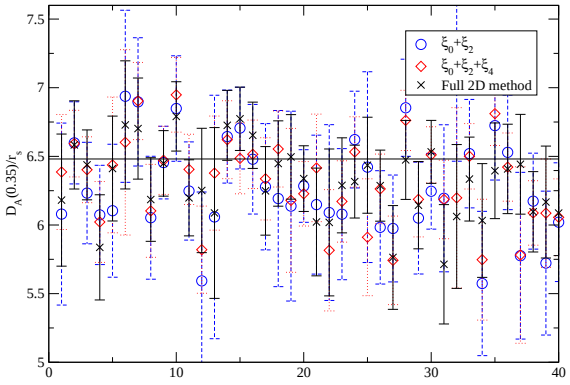

Figure 7. Measurements of the means of $D_A(0.35)r_s(z_d)$ from 40 individual mock catalogs (indexed as 01a to 40a). The blue circles show the measurements using $\hat{\xi}_0+\hat{\xi}_2$. The red dinmonds show the measurements using $\hat{\xi}_0+\hat{\xi}_2+\hat{\xi}_4$. The black crosses show the measurements using full 2D 2PCF method from our previous work. The black line shows the theoretical value computed with the input parameters of the simulations.

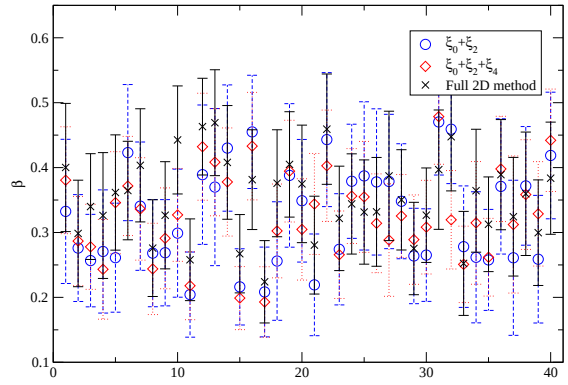

Figure 9. Measurements of the means of β from 40 individual mock catalogs (indexed as 01a to 40a). The blue circles show the measurements using $\hat{\xi}_0+\hat{\xi}_2$. The red dinmonds show the measurements using $\hat{\xi}_0+\hat{\xi}_2+\hat{\xi}_4$. The black crosses show the measurements using full 2D 2PCF method from our previous work.

and 68% confidence level limits of the same parameter set from the measured $\hat{\xi}_0+\hat{\xi}_2+\hat{\xi}_4$ of the correlation function of the SDSS LRG sample for this parameter set. The χ^2 per degree of freedom (χ^2/d.o.f.) is 1.23 for $\hat{\xi}_0+\hat{\xi}_2$ and is 1.06 for $\hat{\xi}_0+\hat{\xi}_2+\hat{\xi}_4$. These are independent of a dark energy model, and obtained without assuming a flat Universe. The measuements from these two methods have deviations which are close to 1σ which occur for some mock catalogs as well (i.e. the result from the 12th mock catalog in Fig. 6). The low measurement of $\Omega_m h^2$ and high measurement of β are found from the mock catalogs, too (i.e. result from the 16th mock catalog in Fig. 8 and Fig. 9). While these cases are rare among the mock catalogs, it is possible that the measurements from the observational data are distorted by some unknown systematic error and not just sample variance. These deviations might provide not only the hints of the appearance of the systematic errors but also the clues for studying them. Here, to be conservative, we use the measurements using $\hat{\xi}_0+\hat{\xi}_2$ as our fiducial results, since $\hat{\xi}_4$ has obvious deviation from the measurement from the mock data (in contrast to $\hat{\xi}_0$, $\hat{\xi}_2$, and $\hat{\xi}_6$, see Figs.1-4).

Table 7 gives the normalized covariance matrix for this parameter set measured using $\hat{\xi}_0+\hat{\xi}_2$. While the measurement of β, 0.44 ± 0.15, is higher than what we expect (i.e $\beta=0.325\pm0.076$ from the mock catalogs using $\hat{\xi}_0+\hat{\xi}_2$), note that there is a negative correlation between β and $\Omega_m h^2$ and the correlation coefficient

	mean	σ	lower	upper
$H(0.35)$	79.6	8.8	70.9	87.8
$D_A(0.35)$	1060	92	970	1150
$\Omega_m h^2$	0.103	0.015	0.088	0.118
β	0.44	0.15	0.29	0.59
$H(0.35)\, r_s(z_d)/c$	0.0435	0.0045	0.0391	0.0477
$D_A(0.35)/r_s(z_d)$	6.44	0.51	5.99	6.90

Table 5. The mean, standard deviation, and the 68% C.L. bounds of $\{H(0.35),\ D_A(0.35),\ \Omega_m h^2,\ \beta,\ H(0.35)\, r_s(z_d)/c,\ D_A(0.35)/r_s(z_d)\}$ from SDSS DR7 LRGs using $\hat{\xi}_0 + \hat{\xi}_2$. The unit of H is $\mathrm{km\,s^{-1}\,Mpc^{-1}}$. The unit of D_A and $r_s(z_d)$ is Mpc.

	mean	σ	lower	upper
$H(0.35)$	87.3	6.7	80.8	93.7
$D_A(0.35)$	1095	59	1037	1153
$\Omega_m h^2$	0.107	0.015	0.093	0.122
β	0.54	0.11	0.44	0.65
$H(0.35)\, r_s(z_d)/c$	0.0472	0.0033	0.0441	0.0503
$D_A(0.35)/r_s(z_d)$	6.75	0.25	6.52	6.98

Table 6. The mean, standard deviation, and the 68% C.L. bounds of $\{H(0.35),\ D_A(0.35),\ \Omega_m h^2,\ \beta,\ H(0.35)\, r_s(z_d)/c,\ D_A(0.35)/r_s(z_d)\}$ from SDSS DR7 LRGs using $\hat{\xi}_0 + \hat{\xi}_2 + \hat{\xi}_4$. The unit of H is $\mathrm{km\,s^{-1}\,Mpc^{-1}}$. The unit of D_A and $r_s(z_d)$ is Mpc.

is -0.2549. Thus the somewhat high β value is mildly correlated with the somewhat low $\Omega_m h^2$ value. The most robust measurements are that of $\{H(0.35)\, r_s(z_d)/c,\ D_A(0.35)/r_s(z_d)\}$, same as in Chuang & Wang (2011). These can be used to combine with other data sets and constraining dark energy and cosmological parameters, see Wang, Chuang & Mukherjee (2012).

Fig. 10 shows one and two-dimensional marginalized contours of the parameters, $\{H(0.35),\ D_A(0.35),\ \Omega_m h^2,\ \beta,\ H(0.35)\, r_s(z_d)/c,\ D_A(0.35)/r_s(z_d)\}$, derived in an MCMC likelihood analysis from the measured $\hat{\xi}_0 + \hat{\xi}_2$ of the SDSS LRG sample.

4.3 Comparison with Previous Work

While we have developed a general method to measure the dark energy and cosmological parameters which could be extracted from the galaxy clustering data alone, we restrict our method now by fixing some parameters to obtain the results for comparison with the previous work by others.

Kazin et al. (2012) present some tests for measuring $H(z)$ and $D_A(z)$ using averaged multipoles of the correlation function from the LasDamas mock catalogs. They assume a larger survey volume ($\sim$ 12 times) by dividing the covariance matrix by $\sqrt{160}$. They use the averaged mulitpoles of the correlation function from the mock catalogs as the theoretical model, which is equivalent to fixing $\Omega_m h^2$, $\Omega_b h^2$, and n_s to the input parameters of the simulations. We fix the damping factor, $k_\star = 0.13\ h\mathrm{Mpc}^{-1}$, and the pairwise peculiar velocity dispersion, $\sigma_v = 300\ \mathrm{s}^{-1}\mathrm{km}$, which give a good fit to the averaged correlation function of the mock catalogs. Corresponding to the bottom panel of fig. 6 in Kazin et al. (2012), we measure the hubble parameter and angular diameter distance by marginalizing over the amplitude of the correlation function and

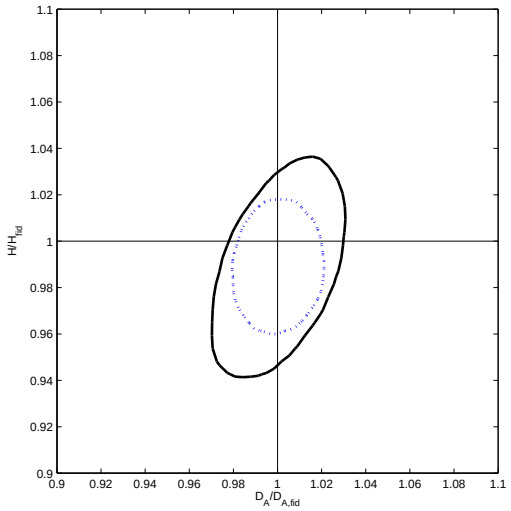

Figure 11. 2D marginalized contours (95% C.L.) for $D_A(z)/D_A^{true}$ and $H(z)/H^{true}$ for the comparison with fig. 6 in Kazin et al. (2012). The black solid contour is measured using $\hat{\xi}_0 + \hat{\xi}_2$ and the blue dotted contour is measured using $\hat{\xi}_0 + \hat{\xi}_2 + \hat{\xi}_4$. Our constraints are similar with the results in Kazin et al. (2012).

the linear redshift distortion parameter and using the scale range, $s = 40 - 150h^{-1}$Mpc. Our results are shown in Fig. 11 which is similar to theirs. The 1-D marginalized uncertainties of $\{H,\ D_A,\ \beta\}$ we measure using $\hat{\xi}_0 + \hat{\xi}_2 + \hat{\xi}_4$ is $\{1.17\%, 0.81\%, 4.45\%\}$ which are similar to their results, $\{1.42\%, 0.76\%, 4.95\%\}$ (the numbers are taken from Fig. 7 in Kazin et al. (2012)). They derive the theoretical multipoles analytically, instead of using the same definition applied to the observational data. In principle, it could introduce biases to the measurments. However, the effect might be minimized since they contruct the theoretical model based on the measured multipoles from the mock catalogs that is equivalent to computing the theoretical multipoles with the same definition applied to the observational data.

Cabre & Gaztanaga (2009) measure β from SDSS DR6 LRG using the normalized quadrupole defined by Eq.(23). To compare with their results, we make similar assumptions, and use monopole-quadrupole method with fixing $\Omega_m = 0.25$, $\Omega_b = 0.045$, $h = 0.72$, $n_s = 0.98$, $k_\star = 0.11$, and $\sigma_v = 300$km/s in the ΛCDM model ($H(0.35)$ and $D_A(0.35)$ would also be fixed accordingly). Considering the scale range, $s = 40 - 100h^{-1}$Mpc, we obtain $\beta = 0.333 \pm 0.055$, in excellent agreement with their meausurement of $\beta = 0.34 \pm 0.05$. Since the definition of the normalized quadrupole includes a integral of monopole with the minimum boundary from $s = 0$, the advantage of using our effective multipole method instead of normailzed quadrupole method is to avoid the distortion from the small scales where the scale dependent uncertainties are not well known. However, the distortion might be negligible compared to the statistical uncertainty of current measurements.

Song et al. (2011) split the same galaxy sample (SDSS DR7 LRG) to two redshift slides and obtained $\beta(z = 0.25) = 0.30^{+0.047}_{-0.048}$ and $\beta(z = 0.38) = 0.39 \pm 0.056$ without considering the geometric distortion. Since we use the whole galaxy sample as one redshift slice, our results are not directly comparable with theirs.

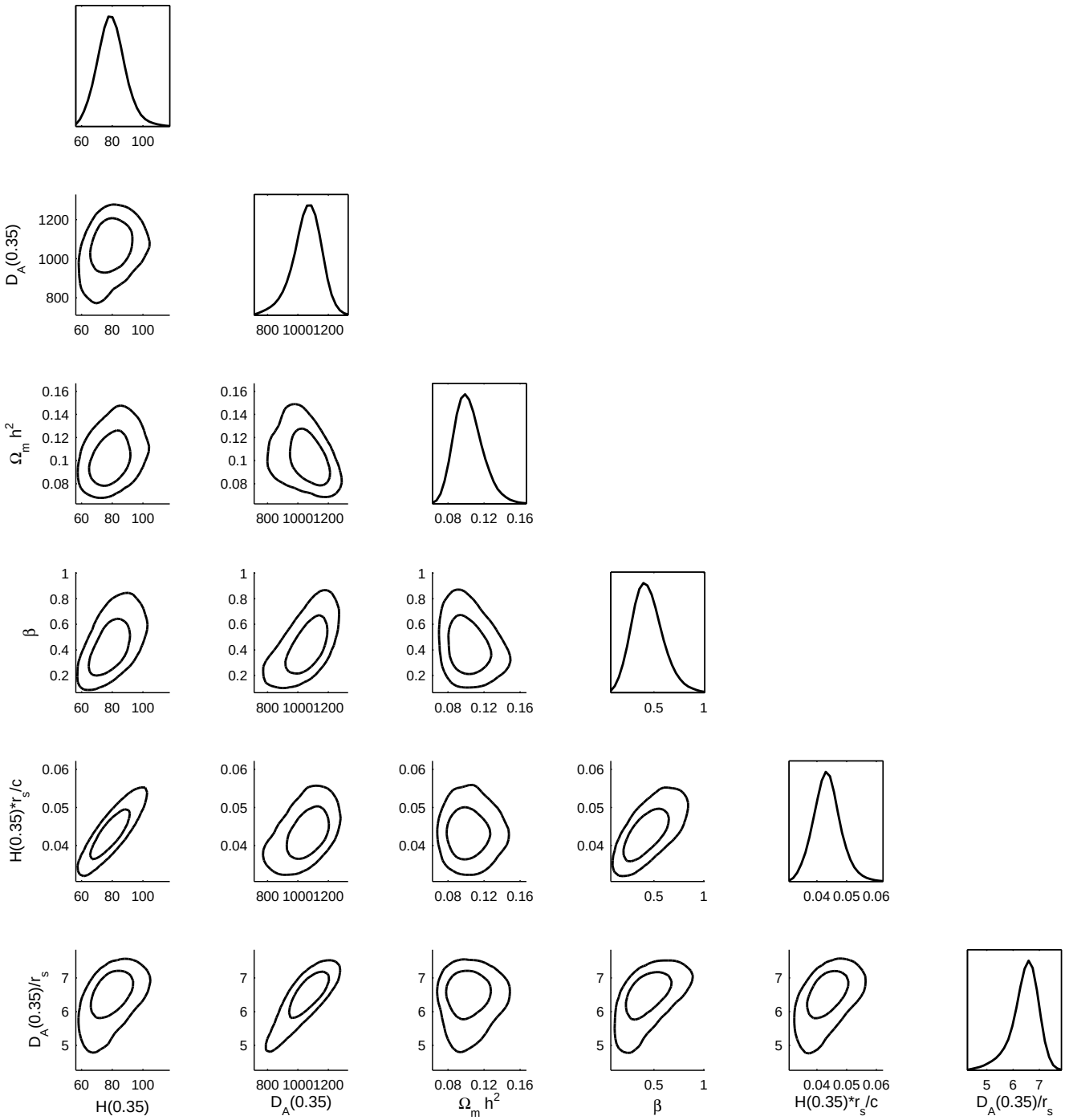

Figure 10. 2D marginalized contours (68% and 95% C.L.) for $\{H(0.35),\ D_A(0.35),\ \Omega_m h^2,\ \beta,\ H(0.35)\, r_s(z_d)/c,\ D_A(0.35)/r_s(z_d)\}$. The diagonal panels represent the marginalized probabilities. The unit of H is $\mathrm{km\,s^{-1}\,Mpc^{-1}}$. The unit of D_A and $r_s(z_d)$ is Mpc.

5 SYSTEMATIC TESTS

Table. 8 shows the systematic tests that we have carried out varying key assumptions made in our analysis. These include the multipoles used, the range of scales used, and the bin size used to calculate the correlation function.

We use the results using $\hat{\xi}_0 + \hat{\xi}_2$ as our fiducial results. We find that the constraints are stronger while using $\hat{\xi}_0 + \hat{\xi}_2 + \hat{\xi}_4$, but using $\hat{\xi}_0 + \hat{\xi}_2 + \hat{\xi}_6$ does not improve the constraints siginicantly. Therefore, it seems that $\hat{\xi}_0 + \hat{\xi}_2 + \hat{\xi}_4$ contains most of the information from the 2D 2PCF. However, since we suspect there is some systematic error for the measurement of $\hat{\xi}_4$ from observational data (see Fig.3), we do not include it for our fiducial results.

We vary the scale chosen and the bin sized used and find the results are basically consistent. However, we find the measurement of $D_A(z)/r_s(z_d)$ is more stable than that of $H(0.35)\, r_s(z_d)/c$. It might indicate the appearance of the systematic error from the measurement of the correlation function in the direction along the line of sight.

	$H(0.35)$	$D_A(0.35)$	$\Omega_m h^2$	β	$H(0.35)\,r_s(z_d)/c$	$D_A(0.35)/r_s(z_d)$
$H(0.35)$	1	0.2669	0.3529	0.5802	0.9259	0.4832
$D_A(0.35)$	0.2669	1	-0.3835	0.6307	0.4586	0.8814
$\Omega_m h^2$	0.3529	-0.3835	1	-0.2549	-0.0057	0.07
β	0.5802	0.6307	-0.2549	1	0.7176	0.575
$H(0.35)\,r_s(z_d)/c$	0.9259	0.4586	-0.0057	0.7176	1	0.4981
$D_A(0.35)/r_s(z_d)$	0.4832	0.8814	0.07	0.575	0.4981	1

Table 7. Normalized covariance matrix of the measured and derived parameters, $\{H(0.35),\ D_A(0.35),\ \Omega_m h^2,\ \beta,\ H(0.35)\,r_s(z_d)/c,\ D_A(0.35)/r_s(z_d)\}$ from SDSS DR7 LRGs using $\hat{\xi}_0 + \hat{\xi}_2$.

	$H(0.35)$	$D_A(0.35)$	$\Omega_m h^2$	β	$H(0.35)\,r_s(z_d)/c$	$D_A(0.35)/r_s(z_d)$
$\hat{\xi}_0 + \hat{\xi}_2$ (fiducial)	$80.0^{+8.2}_{-8.6}$	1063^{+87}_{-85}	0.103 ± 0.015	$0.45^{+0.15}_{-0.14}$	$0.0437^{+0.0041}_{-0.0043}$	$6.48^{+0.44}_{-0.43}$
$\hat{\xi}_0 + \hat{\xi}_2 + \hat{\xi}_4$	87.3 ± 6.4	1095 ± 58	$0.107^{+0.015}_{-0.014}$	0.54 ± 0.11	0.0472 ± 0.0031	$6.75^{+0.24}_{-0.23}$
$\hat{\xi}_0 + \hat{\xi}_2 + \hat{\xi}_6$	$78.5^{+8.7}_{-8.9}$	1025^{+88}_{-82}	0.107 ± 0.016	0.41 ± 0.14	$0.0424^{+0.0044}_{-0.0043}$	6.31 ± 0.49
$30 < s < 120$	$85.1^{+7.8}_{-8.2}$	1072^{+64}_{-62}	0.115 ± 0.014	0.38 ± 0.10	$0.0453^{+0.0037}_{-0.0039}$	$6.71^{+0.31}_{-0.30}$
$50 < s < 120$	$77.5^{+8.2}_{-8.4}$	1034^{+103}_{-109}	$0.101^{+0.019}_{-0.018}$	$0.5^{+0.19}_{-0.18}$	$0.0425^{+0.0038}_{-0.0040}$	$6.27^{+0.55}_{-0.61}$
$40 < s < 110$	$73.5^{+6.7}_{-7.0}$	1064^{+77}_{-76}	0.107 ± 0.015	0.35 ± 0.11	$0.0398^{+0.0031}_{-0.0034}$	$6.54^{+0.41}_{-0.40}$
$40 < s < 130$	$83.5^{+8.3}_{-8.7}$	1082^{+78}_{-75}	0.105 ± 0.015	0.48 ± 0.15	$0.0454^{+0.0041}_{-0.0043}$	$6.63^{+0.37}_{-0.35}$
bin size = 4 h^{-1}Mpc	$77.3^{+7.1}_{-7.2}$	1026^{+86}_{-85}	0.113 ± 0.017	0.39 ± 0.12	0.0413 ± 0.0034	6.39 ± 0.45
bin size = 8 h^{-1}Mpc	$79.1^{+8.1}_{-8.6}$	1065^{+84}_{-78}	0.112 ± 0.017	0.42 ± 0.13	$0.0423^{+0.0039}_{-0.0041}$	$6.62^{+0.41}_{-0.37}$

Table 8. This table shows the systematic tests with using diffirent combination of multipoles, the scale range, and the bin size used. The fiducial results are obtained by considering $\hat{\xi}_0 + \hat{\xi}_2 + \hat{\xi}_4$, the scale range ($40 < s < 120\ h^{-1}$Mpc), and the bin size ($5h^{-1}$Mpc). The other results are calculated with only specified quantities different from the fiducial one. The unit of H is $\mathrm{km\,s^{-1}\,Mpc^{-1}}$. The unit of D_A and $r_s(z_d)$ is Mpc.

6 CONCLUSION AND DISCUSSION

We have demonstrated the feasibility of using multipoles of the correlation function to measure $H(z)$, $D_A(z)$, $\Omega_m h^2$, and β by applying the method to the individual mock catalogs from LasDamas in an MCMC likelihood analysis.

The method we developed is modified from Chuang & Wang (2011) which is the first application of including the geomatric distortion (also known as Alcock-Paczynski test, see Alcock & Paczynski (1979)) on the galaxy clustering data at large scales. We compute the multipoles from the theoretical and observed 2D 2PCF in the same way, thus no more approximation is made besides the distance of any pair of galaxies can be converted with two stretch factors between different models in the redshift range considered.

We have also obtained the constraints for the measured and derived parameters, $\{H(0.35),\ D_A(0.35),\ \Omega_m h^2,\ \beta,\ H(0.35)\,r_s(z_d)/c,\ D_A(0.35)/r_s(z_d)\}$, from the multipoles of the correlation function from the sample of SDSS DR7 LRGs which are summarized by Tables 5 and 6.

We find that while the mean values of estimated parameters remain stable (with rare deviations) for the mock data when higher multipoles are used, this is not true for the SDSS DR7 LRG data. We find $H(0.35)\,r_s(z_d)/c = 0.0437^{+0.0041}_{-0.0043}$ using monopole + quadrupole, and $H(0.35)\,r_s(z_d)/c = 0.0472 \pm 0.0031$ using monopole + quadrupole + hexadecapole. This deviation is caused by the hexadecapole measured from SDSS LRGs deviating from the value expected from the mocks on scales less than about $60\,\mathrm{Mpc}/h$. This suggests that the multipole method can be used to isolate sytematic uncertainties in the data, and provide a useful cross-check of parameter measurements from the full correlation function.

ACKNOWLEDGEMENTS

We are grateful to the LasDamas project for making their mock catalogs publicly available. The computing for this project was performed at the OU Supercomputing Center for Education and Research (OSCER) at the University of Oklahoma (OU). This work used the Extreme Science and Engineering Discovery Environment (XSEDE), which is supported by National Science Foundation grant number OCI-1053575. This work was supported by DOE grant DE-FG02-04ER41305.

Funding for the Sloan Digital Sky Survey (SDSS) has been provided by the Alfred P. Sloan Foundation, the Participating Institutions, the National Aeronautics and Space Administration, the National Science Foundation, the U.S. Department of Energy, the Japanese Monbukagakusho, and the Max Planck Society. The SDSS Web site is http://www.sdss.org/.

The SDSS is managed by the Astrophysical Research Consortium (ARC) for the Participating Institutions. The Participating Institutions are The University of Chicago, Fermilab, the Institute for Advanced Study, the Japan Participation Group, The Johns Hopkins University, Los Alamos National Laboratory, the Max-Planck-Institute for Astronomy (MPIA), the Max-Planck-Institute for Astrophysics (MPA), New Mexico State University, University of Pittsburgh, Princeton University, the United States Naval Observatory, and the University of Washington.

REFERENCES

Abazajian, K. N., *et al.* [SDSS Collaboration], Astrophys. J. Suppl. **182**, 543 (2009) [arXiv:0812.0649 [astro-ph]].
Alcock, C., and Paczynski, B., Nature **281**, 358 (1979).
Bacon DJ, Refregier AR, Ellis RS *MNRAS* 318:625 (2000)
Bennett, C. L., *et al.*, Astrophys. J. Suppl. **148**, 1 (2003)

Blake, C., Glazebrook, K, 2003, ApJ, 594, 665
Blake, C.; Collister, A.; Bridle, S.; and Lahav, O., Mon. Not. Roy. Astron. Soc. **374**, 1527 (2007) [arXiv:astro-ph/0605303].
Blake, C., et al. 2009, MNRAS, 395, 240
Blanton, M. R., *et al.* [SDSS Collaboration], Astron. J. **129**, 2562 (2005) [arXiv:astro-ph/0410166].
Blanton, M. R.; and Roweis, S., Astron. J. **133**, 734 (2007) [arXiv:astro-ph/0606170].
Cabre, A.; and Gaztanaga, E., Mon. Not. Roy. Astron. Soc. **393**, 1183 (2009) [arXiv:0807.2460 [astro-ph]].
Chuang, C. -H.; Wang, Y.; and Hemantha, M. D. P., MNRAS, in press, arXiv:1008.4822 [astro-ph.CO].
Chuang, C. -H. and Wang, Y. arXiv:1102.2251 [astro-ph.CO].
Cimatti, A.; Robberto, M.; Baugh, C. M.; Beckwith, S. V. W.; Content, R.; Daddi, E.; De Lucia, G.; and Garilli B.*et al.*, Exper. Astron. **23**, 39 (2009) [arXiv:0804.4433 [astro-ph]].
Colless, M., *et al.* [The 2DFGRS Collaboration], Mon. Not. Roy. Astron. Soc. **328**, 1039 (2001) [arXiv:astro-ph/0106498].
Colless, M.; Peterson, B. A.; Jackson, C.; Peacock, J. A.; Cole, S.; Norberg, P.; Baldry, I. K.; and Baugh, C. M. *et al.*, astro-ph/0306581.
Eisenstein, D. J.; and Hu, W., Astrophys. J. **496**, 605 (1998) [arXiv:astro-ph/9709112].
Eisenstein, D. J., *et al.* [SDSS Collaboration], Astron. J. **122**, 2267 (2001) [arXiv:astro-ph/0108153].
Eisenstein, D. J., *et al.* [SDSS Collaboration], Astrophys. J. **633**, 560 (2005) [arXiv:astro-ph/0501171].
Eisenstein, D.J., et al., 2011, arXiv:1101.1529v1 [astro-ph.IM]
Fukugita, M.; Ichikawa, T.; Gunn, J. E.; Doi, M.; Shimasaku, K.; and Schneider, D. P., Astron. J. **111**, 1748 (1996).
Gaztanaga, E.; Cabre, A.; and Hui, L. Mon. Not. Roy. Astron. Soc. **399**, 1663 (2009) [arXiv:0807.3551 [astro-ph]].
Gunn, J. E., *et al.* [SDSS Collaboration], Astron. J. **116**, 3040 (1998) [arXiv:astro-ph/9809085].
Gunn, J. E., *et al.* [SDSS Collaboration], Astron. J. **131**, 2332 (2006) [arXiv:astro-ph/0602326].
Hamilton, A. J. S., 1992, APJL, 385, L5
Hutsi, G., arXiv:astro-ph/0507678.
Kaiser, N., Mon. Not. Roy. Astron. Soc. **227**, 1 (1987).
Kaiser N, Wilson G, Luppino GA arXiv:astro-ph/0003338 (2000)
Kazin, E. A., *et al.*, Astrophys. J. **710**, 1444 (2010) [arXiv:0908.2598 [astro-ph.CO]].
Kazin, E. A.; Blanton, M. R.; Scoccimarro, R.; McBride, C. K.; and Berlind, A. A., Astrophys. J. **719**, 1032 (2010) [arXiv:1004.2244 [astro-ph.CO]].
Kazin, E. A.; Sanchez, A. G.; and Blanton, M. R. Mon. Not. Roy. Astron. Soc. **419**, 3223 (2012) [arXiv:1105.2037 [astro-ph.CO]].
Komatsu, E. *et al.* [WMAP Collaboration], Astrophys. J. Suppl. **192**, 18 (2011) [arXiv:1001.4538 [astro-ph.CO]].
Landy, S. D. and Szalay, A. S., Astrophys. J. **412**, 64 (1993).
Landy, S. D., "The Pairwise Velocity Distribution Function of Galaxies in the LCRS, 2dF, Astrophys. J. **567**, L1 (2002) [arXiv:astro-ph/0202130].
Laureijs, R., et al., "Euclid Definition Study Report", arXiv:1110.3193
Lewis, A.; Challinor, A.; and Lasenby, A., Astrophys. J. **538**, 473 (2000) [arXiv:astro-ph/9911177].
Lewis, A. and Bridle, S., Phys. Rev. D **66**, 103511 (2002) [arXiv:astro-ph/0205436].
Martinez, V. J., *et al.*, Astrophys. J. **696**, L93 (2009) [Erratum-ibid. **703**, L184 (2009)] [Astrophys. J. **703**, L184 (2009)] [arXiv:0812.2154 [astro-ph]].
Montesano, F.; Sanchez, A. G.; and Phleps, S., arXiv:1107.4097 [astro-ph.CO].
Okumura, T.; Matsubara, T.; Eisenstein, D. J.; Kayo, I.; Hikage, C.; Szalay, A. S.; and Schneider, D. P., Astrophys. J. **676**, 889 (2008) [arXiv:0711.3640 [astro-ph]].
Padmanabhan, N., *et al.* [SDSS Collaboration], Mon. Not. Roy. Astron. Soc. **378**, 852 (2007) [arXiv:astro-ph/0605302].
Padmanabhan, N.; Xu, X.; Eisenstein, D. J.; Scalzo, R.; Cuesta, A. J.; Mehta, K. T.; and Kazin, E., arXiv:1202.0090 [astro-ph.CO].
Peebles, P. J. E. 1980, The Large-Scale Structure of the Universe (Princeton, NJ: Princeton University Press)
Percival, W. J.; Cole, S.; Eisenstein, D. J.; Nichol, R. C.; Peacock, J. A.; Pope, A. C.; and Szalay, A. S., Mon. Not. Roy. Astron. Soc. **381**, 1053 (2007) [arXiv:0705.3323 [astro-ph]].
Percival, W. J., *et al.*, Mon. Not. Roy. Astron. Soc. **401**, 2148 (2010) [arXiv:0907.1660 [astro-ph.CO]].
Perlmutter, S., *et al.* [Supernova Cosmology Project Collaboration], Astrophys. J. **517**, 565 (1999) [arXiv:astro-ph/9812133].
Press W.H., Teukolsky S,A., Vetterling W.T., Flannery B.P., 1992, Numerical recipes in C. The art of scientific computing, Second edition, Cambridge: University Press.
Ratcliffe, A., et al., 1998, VizieR Online Data Catalog, 730, 417
Reid, B. A.; Percival, W. J.; Eisenstein, D. J.; Verde, L.; Spergel, D. N.; Skibba, R. A.; Bahcall, N. A.; and Budavari, T. *et al.*, Mon. Not. Roy. Astron. Soc. **404**, 60 (2010) [arXiv:0907.1659 [astro-ph.CO]].
Riess, A. G., *et al.* [Supernova Search Team Collaboration], Astron. J. **116**, 1009 (1998) [arXiv:astro-ph/9805201].
Sanchez, A. G.; Crocce, M.; Cabre, A.; Baugh, C. M.; and Gaztanaga, E., arXiv:0901.2570 [astro-ph].
Samushia, L.; Percival, W. J.; and Raccanelli, A., arXiv:1102.1014 [astro-ph.CO].
Saunders, W., *et al.*, Mon. Not. Roy. Astron. Soc. **317**, 55 (2000) [arXiv:astro-ph/0001117].
Seo, H., Eisenstein, D. J., 2003, ApJ, 598, 720
Smith, R. E., *et al.* [The Virgo Consortium Collaboration], Mon. Not. Roy. Astron. Soc. **341**, 1311 (2003) [arXiv:astro-ph/0207664].
Song, Y. -S.; Sabiu, C. G.; Kayo, I.; and Nichol, R. C., JCAP **1105**, 020 (2011) [arXiv:1006.4630 [astro-ph.CO]].
Tegmark, M., *et al.* [SDSS Collaboration], Astrophys. J. **606**, 702 (2004) [arXiv:astro-ph/0310725].
Van Waerbeke, L., et al. *Astron. Astrophys* 358:30 (2000)
Wang, Y., 2006, ApJ, 647, 1
Wang, Y., et al., MNRAS, 409, 737 (2010)
Wang, Y.; Chuang, C. -H.; and Mukherjee, P., Phys. Rev. D **85**, 023517 (2012) [arXiv:1109.3172 [astro-ph.CO]].
Wittman, D. M.; Tyson, J. A.; Kirkmand, D.; Dell'Antonio, I.; Bernstein, G., Nature, 405, 143 (2000)
Zehavi, I., *et al.* [SDSS Collaboration], Astrophys. J. **621**, 22 (2005) [arXiv:astro-ph/0411557].